Imperial College London

Imperial College London

Department of Physics

Using EN4 Analyses for Estimating Trends in Ocean Heat Content

Author:
Jakob Torben

CID: 01413021

Supervisor:
Dr. Arnaud Czaja

Assessor:
Dr. Heather Graven

Project report submitted for the degree of

BSc Physics

October 25, 2020

Word count: 5100

Abstract

The Earth's energy imbalance is responsible for driving the global warming, that is increasingly being witnessed in climate systems worldwide. As most of this energy accumulates in the oceans, Ocean Heat Content (OHC) changes can be used to assess this warming. However, limited ocean observations coverage makes estimating changes in the OHC a significant challenge. In this report, Met Office's EN4 analyses are evaluated for their ability to estimate trends in global OHC change, for 1950-2018. This was again used to quantify the OHC change and its regional variations. The analyses were found to be adequate in estimating OHC, when avoiding time periods and regions of low observational influence as they are heavily influenced by the assumptions made in dealing with regions of no observations. The sampling error was found to be most significant at depths and in the Southern Hemisphere. From 1970-2016, the OHC increased by 24.4×10^{22} J for the 0-2000 m layer, with 74% of the total change in the upper ocean (above 700m). The ocean heat uptake experienced an acceleration around 1997, which is likely linked to a recovery in OHC from the volcanic eruption Mt Pinatubo (1991) masking the acceleration that would have otherwise been observed. In addition, it was likely linked to a reduced sampling error from an increase in observational coverage from the Argo programme. The warming was strongest in the Southern and tropical/subtropical Atlantic Oceans, for periods of both low and high observational influence, revealing a robust footprint of global warming.

Acknowledgements

The project was completed with support from the Space and Atmospheric Physics group in the Department of Physics at Imperial College London. I would like to thank my supervisor Dr. Arnaud Czaja for his excellent support and knowledge throughout the project. Dr. Czaja has been truly inspiring and has significantly developed my interest and knowledge on Oceanography. In addition, I would like to thank my project partner for our successful collaboration in all aspects of the project.

Contents

Chapter 1

Introduction

The Earth has a net positive energy imbalance that drives global warming. The energy imbalance is likely caused by climate forcing from anthropogenic greenhouse gases and aerosols in the atmosphere, but is also affected by natural climate variations and events such as volcanic eruptions [1], [2]. Over 90% of the energy imbalance accumulates in the oceans as increased Ocean Heat Content (OHC) [3]. OHC is much less affected by internal variations and is thus better for observing multi-decadal trends in global temperatures.

The challenges of estimating OHC change lies in the uncertainty associated with historical measurements and unsampled regions of the oceans. Oceanography as a science has been developed in close relation with improvements in observation technologies. Ship measurements were the main source of ocean observations up until 1940 when Mechanical BathyThermographs (MBT) and later expendable BathyThermographs (XBT) started to be used, which drastically increased the number of measurements. However, since they were mainly deployed around trade routes and only measured the upper-oceans (0 to 700 m), the global coverage was still limited, especially in the Southern Hemisphere. MBT and XBT measurements are also subject to systematic errors, however, great progress has been made in applying bias corrections to these measurements [4]. It was not until the Argo era, notably after 2004, that a near-global coverage was reached. Argo is a global network of autonomous profiling floats that is continuously taking ocean measurements between 0 to 2000 m and has become the method of choice for ocean sampling.

The limited global coverage in the pre Argo era, has made OHC estimation with irregular data sampling an active area of research [5], [6]. OHC estimations have a strong dependence on the assumptions made in dealing with unsampled regions and the choice of climatology used [7]. There are several methods used to estimate the OHC in a region with no observations, here the two most common are mentioned. The first method uses a simple area integral of the objective data, which relaxes back to the mean in data-sparse regions and assumes no change in regions of no observations [8]. This method will likely underestimate the OCH change in sparsely sampled regions, such as the Southern Ccean [9]. Whereas the second method uses a weighted area integral from the well-sampled regions weighted by the fraction of the oceans used with observations [10]. In periods of insufficient data coverage the first method significantly underestimates the OHC, while in well-sampled periods both methods suffice [6].

In this report, ocean heat uptake is analysed by using Met Office's EN4 dataset [11]. More specifically, their EN4 analyses from 1950 to 2018 will be evaluated for its ability to estimate OHC change, with a focus on how the historical sampling affects global OHC. Furthermore, the results will be used to analyse the ocean heat uptake and its the geographical variations. Including a discussion on how data coverage, El Niño-Southern Oscillation (ENSO) and volcanic eruptions affect ocean heat uptake. A comparison with similar recent studies will be used to evaluate the validity of the results, more specifically the studies *Levitus 2012* [12] and *Cheng 2017* [5].

Chapter 2

Data and Methods

2.1 EN4 Data Set

EN4 is a collection of quality controlled global ocean observations of temperature and salinity, produced by the Met Office Hadley Centre [11]. It quality controls observation profiles and produces monthly analyses over the period of 1900 to present. Version 4 of the EN series also includes uncertainty estimates of these analyses.

2.1.1 Data Sources

The main data source for EN4 is the World Ocean Database (WOD13) with observations in the period 1900 to 2016. In addition, data compiled from the Arctic Synoptic Basinwide Observations (ASBO) from 1900 to 2008, the Global Temperature and Salinity Profile Project (GTSPP) for 1990 onward and Argo data from the Argo Global Data Assembly Centres for 2000 onward is also used in this project. EN4 is extended on a monthly basis using data from GTSPP and Argo. The collection of different data sources has led to a broad range of measurement platforms in the dataset, as illustrated in Figure 2.1.

Given the limited data available in the early 1900s, this study focuses solely on the period 1950 onward. The ocean profiles are not evenly distributed across the globe from practical reasons such as shipping routes and daylight, weather and ice challenges in high latitude regions. Figure 2.2 shows the geographic coverage for three different periods and the maximum depth of the profile.

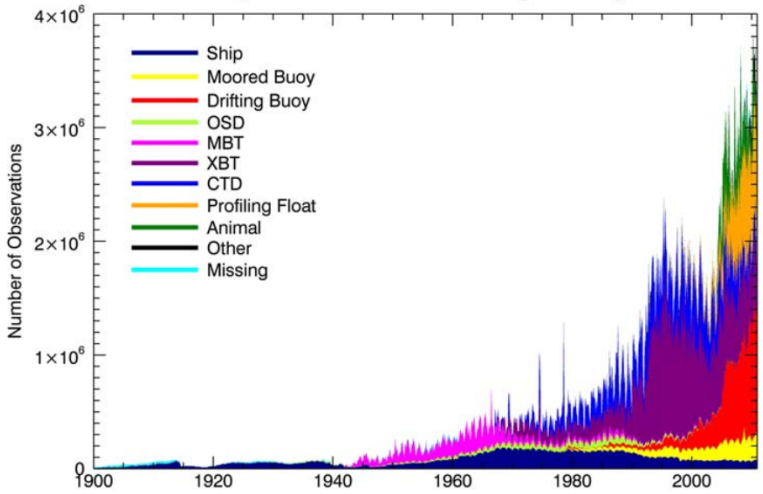

Figure 2.1: Temperature observations by platform type in HadIOD, a database that uses EN4 for subsurface ocean measurements. The Ocean Station Data (OSD) includes low vertical resolution data from both bottle and Conductivity Temperature Depth (CTD) profiles; Mechanical BathyThermograph data (MBT); expendable BathyThermograph (XBT) data; CTD contains high vertical resolution profile data from CTDs and expendable CTDs. Profiling Float is mainly data from the Argo programme. Animal measurements are used to increase coverage in sea-ice regions [13].

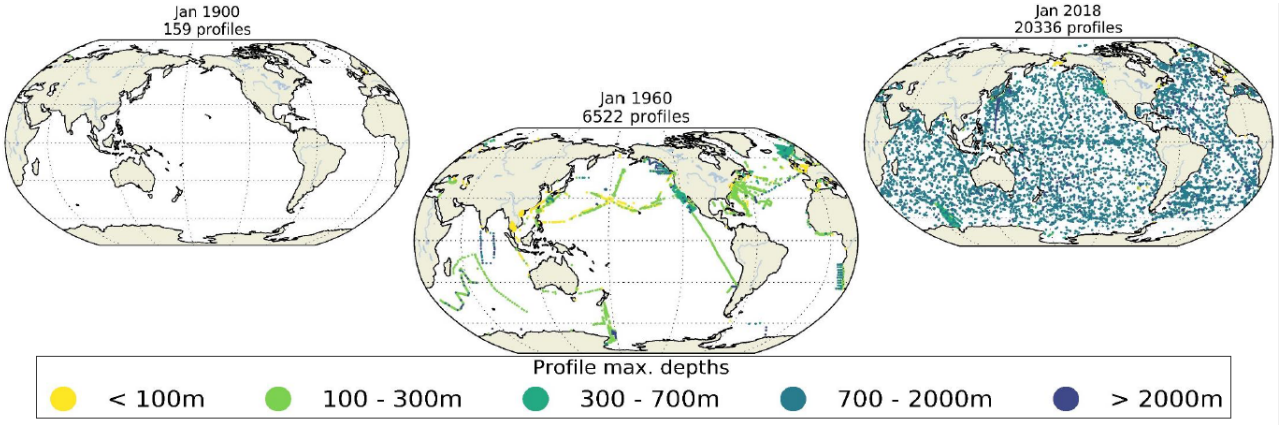

Figure 2.2: Maps of the global coverage of observations used in EN4, in 1900, 1960 and 2018. Notice the limited deep ocean profiles and global coverage in the Southern Hemisphere for 1960 [14].

The map of 1960 illustrates the limited coverage in the Southern Hemisphere and the shallow depths of the profiles. The 2018 map shows the success of the Argo programme in obtaining a uniform global coverage in depths down to 2000 m, with an exclusion of ice-covered regions.

2.1.2 EN4 Processing System

The processes EN4 performs on the data are illustrated in Figure 2.3. They are briefly discussed here, but further details can be found in [11]. Several automatic quality control checks are applied to flag bad quality data. The MBT and XBT profiles are biased with different methods for the different versions used, further details can be found in a paper for the previous version EN3, that describes the biases applied [15].

To create the analyses, a persistence-based forecast of the ocean state from the previous month's objective analyses are compared with the quality controlled profiles from the month being analysed. Where the monthly objective analyses are created from the quality controlled data. The persistence-based forecast in month i is calculated as follows:

$$\mathbf{x}_i^f = \mathbf{x}_i^c + \alpha \left(\mathbf{x}_{i-1}^a - \mathbf{x}_{i-1}^c \right), \tag{2.1}$$

where $\mathbf{x}_i^f$ is the forecast generated from the climatology $\mathbf{x}_i^c$ in the month used plus the anomalies of the previous month $\mathbf{x}_{i-1}^a$ minus the climatology $\mathbf{x}_{i-1}^c$ for that month. The climatology represents an average over 1971-2010, which was determined from a smoothed objective analyses from EN2, which in turn used World Ocean Atlas 1998 as its climatology.

The authors of EN4's paper noted that analyses will relax to climatology in regions of no observations. "Care must therefore be taken if using the analyses for applications such as identifying trends in temperature or salinity,because a trend may be unrealistic if analysing periods when there were no observations" [11]. This method lies in between the two methods mentioned in the introduction, as it does not assume no anomaly in regions of no observations, but rather uses the climatology. In regions of no observations, the climatology are also subject to sampling error and acts a mean state over a larger region.

New to version 4 of the EN datasets are uncertainty estimates on the analyses. The uncertainties are estimated by performing an observation influence analysis that can be used to infer the analysis error variance. Further details on the methods can be found in the EN4 paper [11]. Using this method, uncertainties on the analyses are provided down to around 1000 m for 90% of the ocean temperatures.

2.2 Events Affecting Ocean Heat Content

In order to analyse to what extent events such as the El Niño Southern Oscillation (ENSO) and volcanic eruptions have affected ocean heat uptake, the OHC time series was compared to data on the events. In the event of a volcanic eruption, aerosols ejected into the stratosphere scatters incoming solar radiation, which causes a rapid cooling of the atmosphere. To quantify the effect of a volcanic eruption, the global average optical depth from NASA Goddard Institute for Space Studies was used. The analysis will be compared to a study that uses

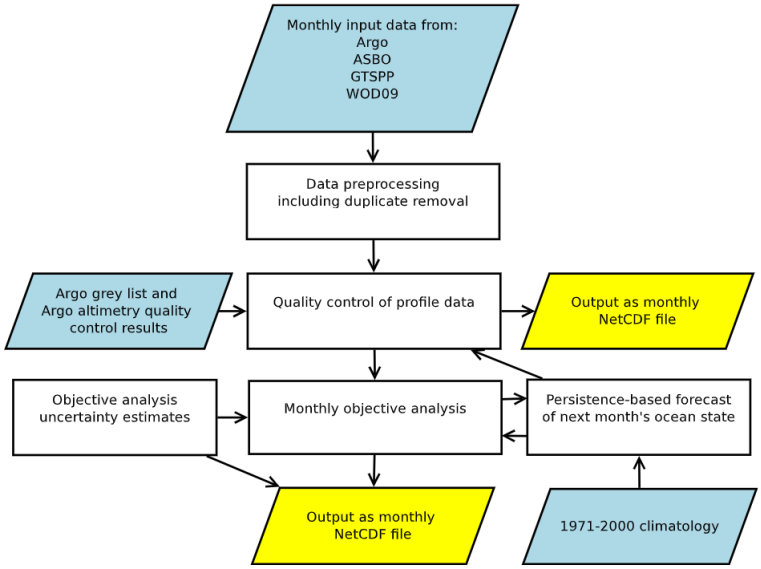

Figure 2.3: Flow of EN4's data processing system. Adapted from [11].

OHC and a specially designed climate model simulation to isolate the effect of a volcaninc forcing [2].

ENSO events are the largest interannual perturbations to Earth's climate system and have major effects on the year-to-year variations in OHC. As the largest changes reside in the tropical Pacific Ocean, analyses of ENSO events prior to Argo are somewhat limited by observations. For completeness, surface temperatures from the HadCRUT4 dataset was used to support the analysis of how ENSO and volcanic eruptions affect OHC [16].

2.3 Methods for Estimating Ocean Heat Content

OHC is calculated using the potential temperature anomalies Θ between depths h_1 and h_2:

$$OHC = \int_{h_1}^{h_2} \rho C_p \Theta dz \tag{2.2}$$

where ρ, C_p is the density and specific heat capacity of seawater, respectively. For the purpose of this report, ρ and C_p are treated as constants, while in reality they vary with temperature and salinity.

Temperature data was extracted from the EN.4.2.1 analyses with Gouretski 2010 corrections over the time period 1950 to 2018. The corrections are mainly biases to MBT and XBT measurements [17]. EN4 analyses comes in the format of 1°-by-1° gridded cells with 42 unevenly spaced depth levels of high resolution at shallow depths and vice versa. To estimate the OHC, temperature data was interpolated using a cubic spline in steps of 1 m and used in Equation 2.2, multiplied by its area. To account for numerical rounding errors, all checks for zero were replaced with a small number above the machine precision. Given the size and structure of the data set, the calculations were performed in parallel to reduce the computation time, by utilising the multi-dimensional optimised Python package 'xarray'.

The anomaly of the OHC time series was found by subtracting the mean of the period 1950 to 2002, where the data was within one standard deviation from the starting to point. To remove seasonal variations in the time series, moving averages (backwards and ahead in time) of one and three years were used. This removes an equivalent number of years to the start and end time of the time series.

Geographical variations were analysed using a linear trend of a one year moving average OHC time series for each grid cell. The covariance of the linear fit was used to find the error on the trend, which can identify regions where OHC differs from a linear relationship. A parabolic fit was also tested, but was found inferior to a linear fit, as it had higher errors and unstable behaviour in determining the sign of the curvature. To further aid the analyses, a zonal-mean OHC change was computed by comparing five year averages for different periods, for one-degree latitude belts for 50 m-thick depth layers. The zonal-mean adds the dimension of depth to the analysis of the geographic variations of ocean heat uptake.

Chapter 3

Results and Discussion

3.1 Global Ocean Heat Content Change

Figure 3.1 shows an estimate of the global OHC change in the period 1953 to 2016 for different depth layers down to 2000 m. Between 1970 and 2016, the OHC increased by $24.4 \times 10^{22}\,J$. There is a significant acceleration of ocean heat uptake around year 1997; in the period 1970 to 1997 the annualised increase of a linear trend was $0.03 \times 10^{22}\,J\,year^{-1}$ (corresponding to a rate of $0.04\,W\,m^{-2}$ per unit area), compared to $1.15 \times 10^{22}\,J\,year^{-1}$ ($0.71\,W\,m^{-2}$ per unit area) after 1997. The latter period is consistent with a recent estimate of Earth's energy imbalance (EEI) of $0.9 \pm 0.3\,W\,m^{-2}$ for 2005–14, when taking into account that only the upper ocean is considered and some of the energy does not end up in the ocean [18]. Between the time periods the rate of ocean heat uptake increases by over 17 times, this acceleration is most probably related to the increasing EEI with time.

3.1.1 Events Affecting OHC Change

Aerosols ejected into the stratosphere during a volcanic eruption scatter the incoming radiation, which in turn reduces the EEI. This causes a rapid cooling of the atmosphere, which again affects the ocean heat uptake. To evaluate the effect this has on the OHC, Figure 3.2 shows the upper ocean layers, which is where events such as these have the largest effect. The magnitude of the impact the aerosols have on the EEI is quantified by the global mean optical depth on a scale between 0 to 1. In the time period considered, there have been three major volcanic eruptions, Mt Agung (Indonesia, 1963), El Chichon (Mexico, 1982) and Mt Pinatubo (Philippines, 1991).

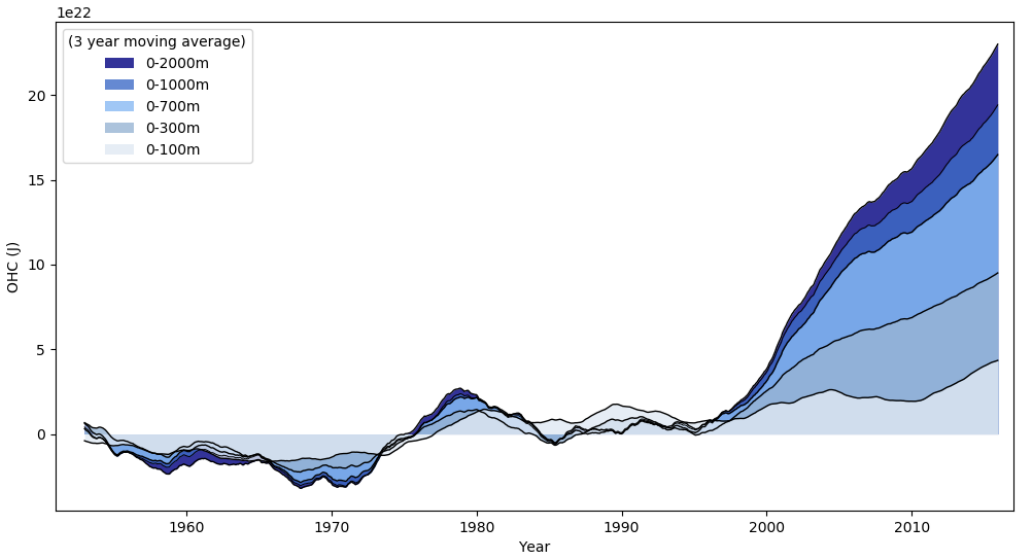

Figure 3.1: Time series of ocean heat content for the 0-100, 0-300, 0-700, 0-1000, 0-2000 m layers. The seasonal variations have been smoothed with a 3 year moving average.

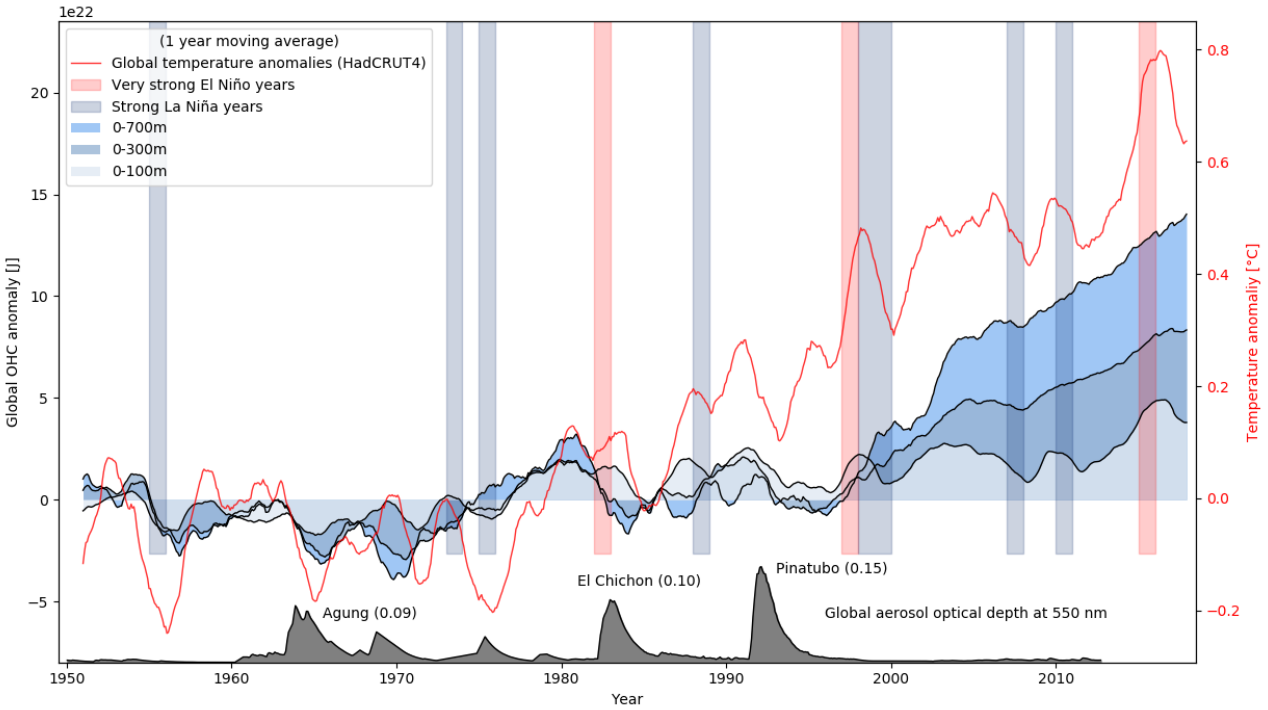

Figure 3.2: Time series of ocean heat content for the 0-100, 0-300, 0-700 m layers. The seasonal variations have been smoothed with a 1 year moving average, to capture shorter fluctuations. The sea surface temperature anomaly is represented by a red dotted line [16] and the mean global optical depth at 550 nm is shown in grey on a scale from 0 to 1 [20]. Very strong El Niño years and strong La Niña years are shown in red and blue, respectively.

Mt Pinatubo had the largest effect on the EEI, with an optical depth of 0.15. It is also the volcanic eruption with the best observations of aerosols and OHC and so will therefore be used to analyse the effect. Following the eruption, the global surface temperature drops rapidly by about $0.4\,°C$. This reduction further manifests into the ocean, which is most probably linked to the observed decrease in OHC. The OHC falls rapidly for over a year, and does not make a complete recovery until around year 2000. The observations are clearly also affected by the El Niño-Southern Oscillation (ENSO) event of 1997/98.

In a study that compared the change in OHC following Mt Pinatubo to climate model simulations, the effect of the eruption was estimated to a decrease of around $3 \times 10^{22}\,J$ in OHC [2]. Furthermore, a recent study, that compared altimeter data to specially designed climate model simulations, showed that the eruption likely masked the acceleration that would have otherwise occurred [19]. It is therefore likely that the recent acceleration observed in the global OHC is partly due to the recovery from the eruption.

Figure 3.2 also shows the very strong ENSO events in the given period. ENSO events are the largest inter-annual perturbations to Earth's climate system and have major effects on the year-to-year variations in OHC. During an ENSO event the thermal structure of equatorial Pacific has large deviations from climatology. As a consequence, EN4 will not be a good measure of the impact of ENSO in periods and regions of no observations, which applies mainly to the pre Argo era. As there is no consensus on the role of ENSO events on Earth's energy budget and large variations between different events, the overall effect on OHC is still uncertain.

During an El Niño, heat is being redistributed adiabatically in the oceans and diabetically into the atmosphere. This causes a cooling in the Pacific, but a warming in other basins. In a recent study on Argo data, the Pacific cooling was found to be largely offset by a warming in the Indian and Atlantic Oceans, giving a weak but robust net global ocean cooling during and after El Niño [21]. This pattern can be observed in Figure 3.2 of a decrease of OHC in the shallow layers, accompanied with an increase in the surface temperature. Although, ENSO events have a limited effect on the overall trend of OHC, it is still important to acknowledge its significant short-term effect on OHC.

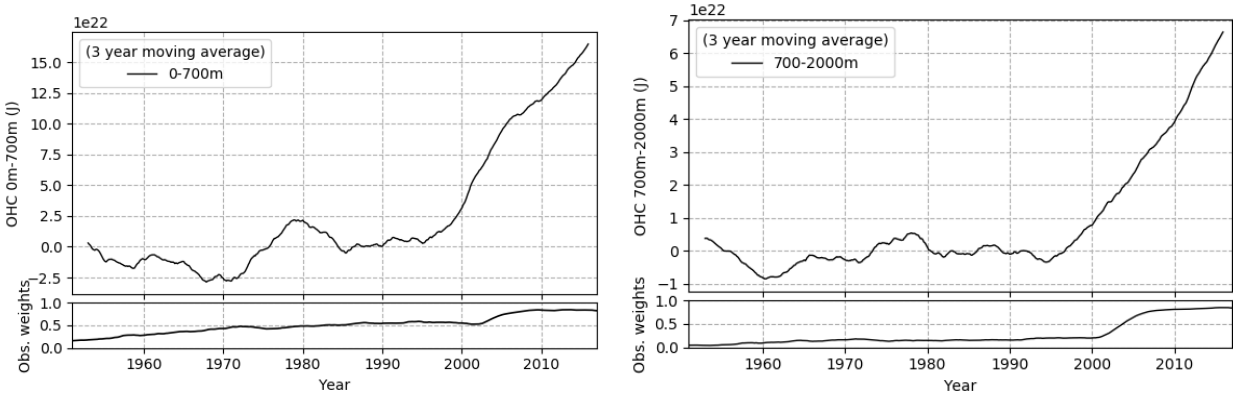

(a) 0-700 m (b) 700-2000 m

Figure 3.3: Time series of ocean heat content change for different depth layers and the mean observational weight used in forming the analyses. The EN4 analyses uncertainty have been plotted for the 0 to 700 m plot, but is insignificantly small when propagating the errors of the global sum. Seasonal variations are smoothed with a 3 year moving average.

	1970 - 2015	1970 - 1997	1997 - 2015
Depth layer (m)	$W\,m^{-2}$	$W\,m^{-2}$	$W\,m^{-2}$
0-2000	0.192 ± 0.005	0.038 ± 0.006	0.711 ± 0.005
0-700	0.221 ± 0.005	0.041 ± 0.005	0.503 ± 0.006
700-2000	0.072 ± 0.002	-0.005 ± 0.001	0.212 ± 0.001

Table 3.1: Table of the global rate of ocean heat content increase per unit area, in the entire considered period and before and after 1997 for different depth layers. The uncertainties have been estimated from the covariance of the linear fit, and acts as measure of how well it follows a linear trend.

3.1.2 Depth Layers

Figure 3.1 shows that a large part of the OHC increase in the last decades has occurred in the upper 700 m layer of the world ocean. To evaluate the ocean heat uptake of the different layers, Figure 3.3 compares the OHC of layer 0 to 700 m and 700 to 2000 m. It also shows the global mean observation weights used in calculating EN4's analyses, as discussed in Section 2.1.2. In time periods of low observational influence the analyses relaxes to climatology, which may have unrealistic trends. To avoid this, the annualised trends are limited to the time period 1970 to 2016, where the mean observation weights are above 0.5 for the upper ocean. Several uncertainty studies indicate that the historical observations begin to be reasonably suited from 1970 onward [6], [22]. The Figure shows that the OHC increased more steadily in the upper ocean, but remains relative flat until around 1997 for the 700 to 2000 m depth layer. In the period 1970 to 2016, 74% of the OHC change happened in the 0 to 700 m depth layer of the total 0 to 2000 m layer.

The annualised rates of the different depth layers are summarised in Table 3.1. Between 1970-1997 and 1997-2016, the ocean heat uptake is accelerating (by 12 times for 0-700m), where the deeper layer goes from no OHC change to a significant change. This acceleration is probably linked to the increasing EEI with time and the recovery in OHC from Mt Pinatubo, as mentioned in the preceding section.

3.1.3 Observations and Uncertainty

The non existent heating in the deeper oceans before 1997 is contradicting the net positive EEI since the 1960s [1]. There are several hypothesis as to why this is the case. For example, the warming in the 1960s is small and can be be influenced by sampling error or potentially the strong warming in the upper ocean does not penetrate to depths below 700 m [5]. Figure 3.3 shows that the mean observational weights of the deeper layer 700 to 2000 m are below 0.2 up until year 2000. In periods of low observational influence, EN4 analyses are strongly influenced by the choice of climatology, which makes it unreliable in representing OHC in the deeper ocean layers [7]. There also appears to be a correlation between the observational influence and the increase in OHC, which suggests that the increase in OHC after 1997 could be consequence of better observations in the deeper ocean.

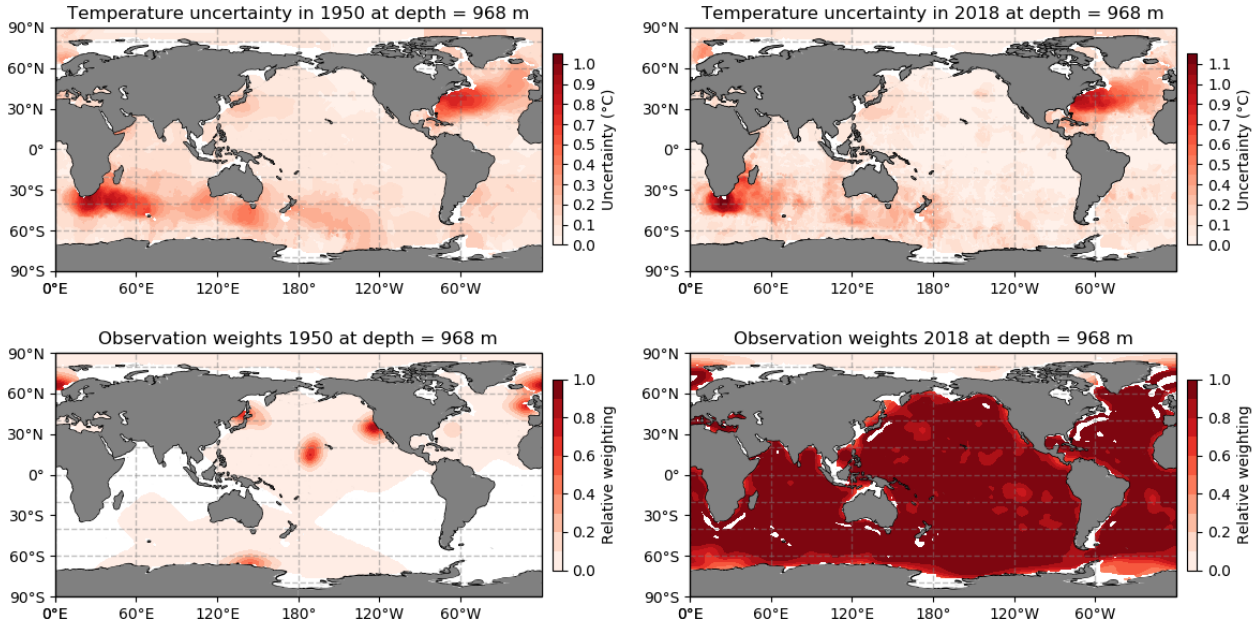

Figure 3.4: Upper row: Temperature uncertainty from EN4 analyses at a depth of 968 m, for 1950 and 2018. Notice the large uncertainties in the regions of high variability, which are likely overestimated [11]. Bottom row: Observational weights used in forming the analyses. Notice the low observational influence in 1950, especially in the Southern Hemisphere.

EN4 analyses also includes uncertainty estimates based on the observational influence and error variance. Figure 3.4 shows the uncertainty and observational weights at a depth of 968 m, plotted on a map in year 1950 and 2018. It shows the evolution of the observational influence, going from large regions with an almost zero weighting in the Southern Hemisphere in 1950, to a close to homogeneous weighting in 2018, mainly thanks to the efforts of the ARGO programme. It also shows that the uncertainties are large in regions of high variations, as noted in the EN4 paper [11]. However, in the regions of low observational coverage, the uncertainties are lower than expected. The authors the EN4 paper warned that the uncertainty is likely underestimated at depth as the error variance of the climatology is underestimated.

For the depth layer 0 to 700 m in Figure 3.3, the uncertainty is plotted as bands. However, when propagating the errors of the global sum, they are insignificantly small. When also taking into account the likely underestimation mentioned above, not much weight is placed on using the uncertainty on global OHC change. Other studies have derived methods of estimating uncertainty on the global OHC [5], [12].

3.2 Regional Variations in Ocean Heat Content

Regional variations in OHC are of great interest as a method to explain the mechanism behind the OHC changes. Figure 3.5a shows a map of the linear trend of the OHC of 0 to 2000 m for every grid cell over the period 1950 to 2018. The error on the linear fit was highest in regions of high variability, which is as expected, given the larger variations and uncertainty on the analyses. During the period, 79% of the grid cells experienced a warming, which sums up to a global average rate of $0.192 W\, m^{-2}$ per unit area. It shows that most regions experienced a warming in the period, with an exception of the East Pacific and North Atlantic Oceans. It is well known that the North Atlantic was cooling between the 1970s and 1995, accompanied with an opposite trend in subtropical Atlantic Ocean [23]. Southern Ocean experiences the most prevalent heating, which agrees with IPCC's recent report where it estimates its contribution to increasing the OHC of $35\% - 43\%$ [24].

To further investigate the regional variations by depth, Figure 3.5b shows a zonally integrated OHC for the world, computed by 50m depth layers, of the difference between the 5-year averages 2014-18 and 1950-54. It shows that most regions experienced a warming in the period, with strongest warming found near the sea surface. In the Southern Hemisphere, there is a strong warming that penetrates to depths of at least

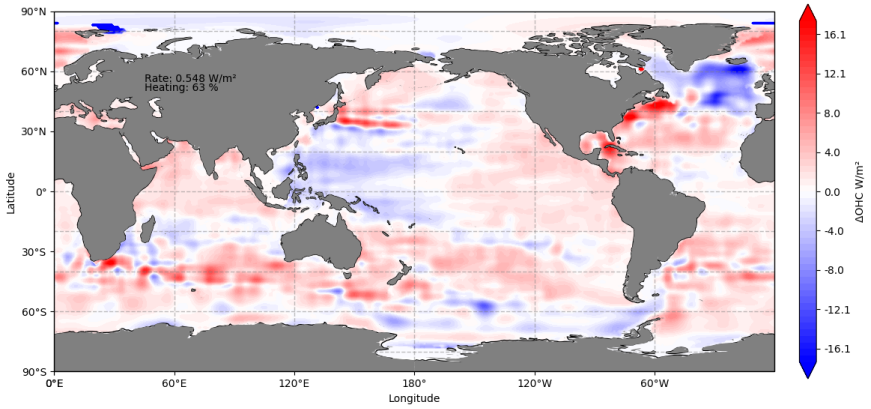

(a) Contour map of linear trend of every grid cell. The total rate is found from summing up all cells and dividing by the global area. The percentage of heating is the fraction of cells that has a net positive change, excluding the continents.

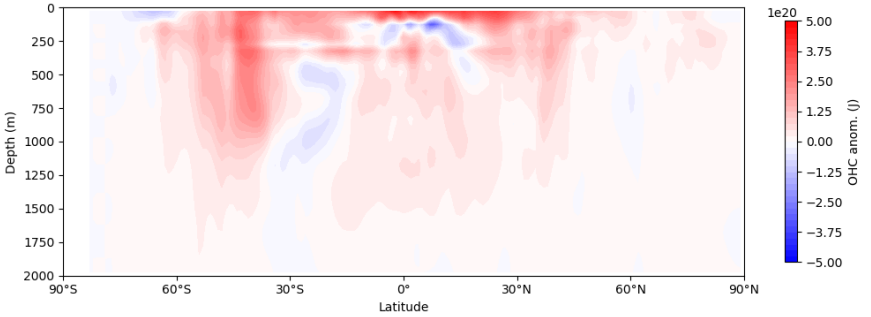

(b) Difference in 5 year averages at the start and end of the time period of the zonally integrated heat content of the world ocean by 1° latitude belts for 50 m depth layers.

Figure 3.5: Regional variations in the period 1950 to 2018.

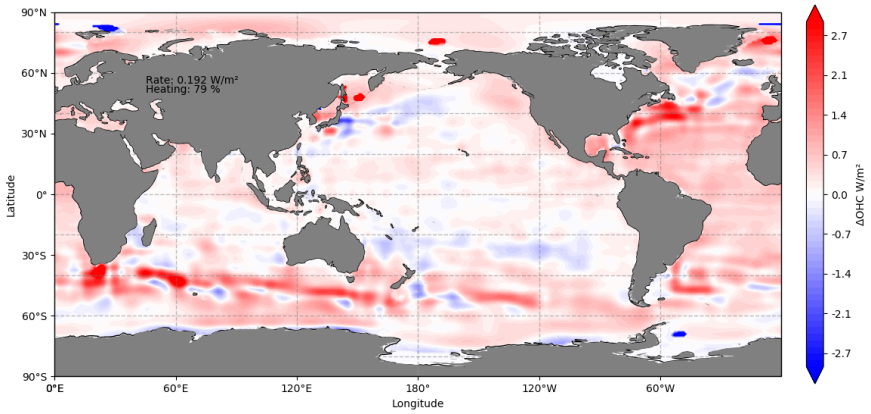

(a) Contour map of linear trend of every grid cell. The total rate is found from summing up all cells and dividing by the global area. The percentage of heating is the fraction of cells that has a net positive change, excluding the continents.

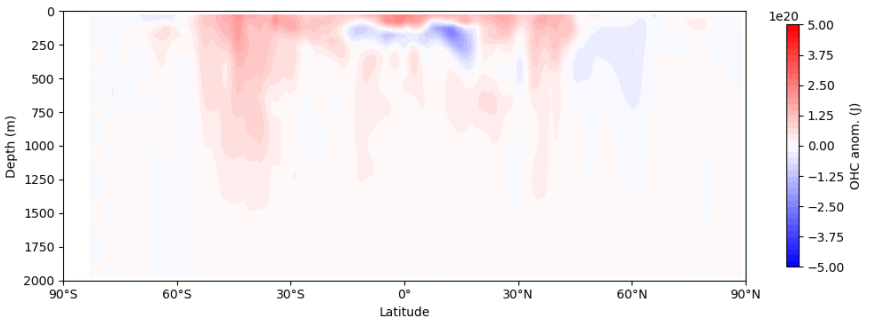

(b) Difference in 5 year averages at the start and end of the time period of the zonally integrated heat content of the world ocean by 1° latitude belts for 50 m depth layers.

Figure 3.6: Regional variations in the better sampled period 2004 to 2018

1000 m, accompanied with a subsurface cooling of the Indian Ocean. The warming of the Southern Ocean in this period is well documented by *Gille 2008* [9]. The zonal plot shows that the cooling of the East Pacific is limited to shallow depths. It is important to bear in mind the sparse observations in the beginning of this period, especially for the Southern Ocean, which causes an attenuation of the anomalies in creating the analyses.

Figure 3.6 shows an equivalent plot, but for the period 2004 to 2018. This period was intentionally chosen in order to assess if the same regional trends are witnessed in the better sampled Argo era. Note that the result will also be affected by the El Niño event of 2015/16 in this period. From the linear trends of the map, 55% of the grid cells experienced warming, which sums up to an average global warming rate of $0.625\,W\,m^{-2}$. In other words, fewer regions are experiencing warming, but the overall warming rate is still higher. Based on the Figure 3.6a, the smaller percentage of warming cells is largely due to the relatively unchanged Pacific Ocean. While the higher warming rate is likely a result of the strong warming in the Southern Ocean and Atlantic.

Since the warming of the Southern Ocean and Equatorial and South Atlantic Ocean still holds for the better sampled period of 2004-18, it is likely that the warming is real and not just a sampling error. There are several theories on the mechanisms behind the warming. A study suggest that the Atlantic meridional overturning circulation, a system of ocean currents that transports warm water from the tropics northwards into the North Atlantic, has been weakening during the 2000s causing the recent warming [25]. Regardless of the mechanism, the Southern and Atlantic Oceans have experienced significant warming since 1950, demonstrating a robust footprint of global warming.

3.3 Comparison to Other Studies

To further evaluate EN4's ability to estimate OHC, the values can be checked against similar studies. The study by *Levitus 2012* found an OHC change in the 0 - 2000 m depth layer of $24.0 \pm 1.9 \times 10^{22}\,J$ in the period 1955-2010 [12]. This study used a similar method as EN4, but with a first guess of zero, which makes it relax to zero anomalies in regions of no observations. This is a similar result to the estimate obtained in this report of $22.3 \times 10^{22}\,J$ for the time period 1953 - 2016. In another study *Cheng 2017*, a different approach was used to deal with regions of low observation data, where it used Argo data colocated with locations of earlier ocean observation to minimise the sampling error. It estimated the OHC change in the 0 to 2000 m depth layer of $29.2 \pm 6.1 \times 10^{22}\,J$ for the 1960 to 2015. For the same period, the updated *Levitus 2012* estimate has a similar, but slightly lower estimate, which illustrates the sensitivity to the method of dealing with regions of no observations, where *Levitus 2012* is likely underestimating the OHC change by assuming no anomalies in regions of no observations.

These literature values show that the OHC change estimate from EN4's analyses is comparable to other studies, but is underestimating the overall change. The *Cheng 2017* study also reported warming rates of the depth layer 0 - 700 m of $0.09 \pm 0.05\,W\,m^{-2}$ for the period 1960-91 and $0.61 \pm 0.03\,W\,m^{-2}$ a warming trend four times stronger than 1960-91. A similar acceleration was observed in the estimates provided in this report of $0.061 \pm 0.004\,W\,m^{-2}$ and $0.456 \pm 0.005\,W\,m^{-2}$, a warming trend seven times stronger than 1960-91. Again the estimate provided here matches the behaviour, but underestimates the overall trend. The uncertainties of the estimates provided here are unrealistically small, compared to the literature values, as they only refer to error in the fit, which clearly underestimates the underlying uncertainty in the data. Since the warming rate of the OHC estimate provided here is accelerating faster than in the *Cheng 2017* study, it is possible that the underestimation is partly due to EN4's behaviour in poorly sampled periods.

The comparison shows that the EN4 analyses do represent the major trends, but are unreliable in periods of little observations. This is a common theme in OHC estimation and is not an isolated problem for EN4. It is therefore better to use objective observations in regions that have poor sampling and apply appropriate methods. This gives a better overview over the assumptions that are made in dealing with regions of no observations, which have a large effect on the OHC estimate.

Chapter 4

Conclusion

Accurate and reliable estimates of Ocean Heat Content (OHC) are highly valuable in understanding the effect of climate change. It improves our understanding of the mechanisms of variations in OHC driven by both external forcing and internal variations. A significant challenge of oceanography is the limitation imposed by observations in historic measurements. Improved data coverage in the Argo era, specifically after 2004, has greatly improved our estimates of OHC and allowed reanalyses of historic measurements.

This study uses Met Office's EN4 analyses in estimating the change in OHC over the period 1950 to 2018. The analyses were found to be unreliable in periods of low observational influence, as the analyses relaxes to climatology in absence of observations. This caused an underestimation of the increase in OHC, compared to other studies. Sampling error was most prevalent at depths below 700 m, as there are limited observations up until the Argo era. In the period 1970 to 2015, for which the OHC is less prone sampling error, the change in OHC for the depth layer 0 to 2000m was found to be $24.4 \times 10^{22}\,J$. 74% of the OHC change happened in the upper ocean (0 - 700 m), which may be partly due to the sampling error at depths.

The ocean heat uptake accelerated around year 1997, which was accompanied by a rapidly increasing observational influence, from the Argo programme beginning in 2000. It is possible that part of this acceleration is due to the sampling error mentioned above, especially as more observations were obtained at depths. Furthermore, the change in OHC was clearly affected by the volcanic eruption Mt Pinatubo in 1991. The eruption caused a global cooling of the ocean of about $3 \times 10^{22}\,J$ and did not recover completely until about year 2000. It is likely that this event masked the acceleration that would have otherwise happened and caused a rapid acceleration after its recovery. In addition, the OHC change showed that El Niño-Southern Oscillation events affect the year-to-year variations in OHC, but have a less severe impact on the long term trends.

Nearly all regions warmed at all latitudes between 1950 and 2018, except in the North Atlantic and East Pacific Oceans. The warming was strongest near the sea surface. The Southern Ocean and tropical/subtropical Atlantic experienced the strongest warming, with the Southern Ocean being the largest single contributor. Some of the Southern warming could be a result of greater numbers of ocean observations at later times. However, the warming was also observed in the Argo era, revealing a robust footprint of global warming.

In conclusion, the EN4 analyses are adequate for estimating the change in OHC, when special care is taken in time periods and regions of low observational influence. In regions such as these, it is good practice to use use objective observations and apply appropriate methods as it gives a better overview of the assumptions made in dealing with regions of no observations. When this flaw was taken into account, this study found a robust warming of the upper oceans, between 1970 and 2015. An extension of this report would include a further analysis of the uncertainties associated with creating the analyses, to provide realistic uncertainties on the OHC estimates. In addition, only the depth layer between 0 to 2000 m was considered, which leaves out a large part of the oceans. However, depths below 2000 m does likely not contribute a great deal to the overall change in OHC and analysing them would be prone the significant sampling error.

Bibliography

[1] M. Rhein, S. Rintoul, S. Aoki, E. Campos, D. Chambers, R. Feely, S. Gulev, G. Johnson, S. Josey, A. Kostianoy, C. Mauritzen, D. Roemmich, L. Talley, and F. Wang, *Observations: Ocean.* Cambridge, United Kingdom and New York, NY, USA: Cambridge University Press, 2013.

[2] J. Church, N. White, and J. Arblaster, "Significant decadal-scale impact of volcanic eruptions on sea level and ocean heat content," *Nature*, vol. 438, pp. 74–7, 12 2005.

[3] J. A. Church, N. J. White, L. F. Konikow, C. M. Domingues, J. G. Cogley, E. Rignot, J. M. Gregory, M. R. v. d. Broeke, A. J. Monaghan, and I. Velicogna, "Revisiting the Earth's sea-level and energy budgets from 1961 to 2008," *Geophysical Research Letters*, vol. 38, no. 18, 9 2011.

[4] L. Cheng, J. Abraham, G. Goni, T. Boyer, S. Wijffels, R. Cowley, V. Gouretski, F. Reseghetti, S. Kizu, S. Dong, F. Bringas, M. Goes, L. Houpert, J. Sprintall, and J. Zhu, "Xbt science: Assessment of instrumental biases and errors," *Bulletin of the American Meteorological Society*, vol. 97, no. 6, pp. 924–933, 2016.

[5] L. Cheng, K. E. Trenberth, J. Fasullo, T. Boyer, J. Abraham, and J. Zhu, "Improved estimates of ocean heat content from 1960 to 2015," *Science Advances*, vol. 3, no. 3, 2017.

[6] J. M. Lyman and G. C. Johnson, "Estimating annual global upper-ocean heat content anomalies despite irregular in situ ocean sampling," *Journal of Climate*, vol. 21, no. 21, pp. 5629–5641, 2008.

[7] ——, "Estimating global ocean heat content changes in the upper 1800 m since 1950 and the influence of climatology choice," *Journal of Climate*, vol. 27, no. 5, pp. 1945–1957, 2014.

[8] S. Levitus, J. Antonov, and T. Boyer, "Warming of the world ocean, 1955–2003," *Geophysical Research Letters*, 2005.

[9] S. T. Gille, "Decadal-scale temperature trends in the southern hemisphere ocean," *Journal of Climate*, vol. 21, no. 18, pp. 4749–4765, 2008.

[10] J. M. Gregory, H. T. Banks, P. A. Stott, J. A. Lowe, and M. D. Palmer, "Simulated and observed decadal variability in ocean heat content," *Geophysical Research Letters*, vol. 31, no. 15, 2004.

[11] S. A. Good, M. J. Martin, and N. A. Rayner, "En4: Quality controlled ocean temperature and salinity profiles and monthly objective analyses with uncertainty estimates," *Journal of Geophysical Research: Oceans*, vol. 118, no. 12, pp. 6704–6716, 2013.

[12] S. Levitus, J. I. Antonov, T. P. Boyer, O. K. Baranova, H. E. Garcia, R. A. Locarnini, A. V. Mishonov, J. R. Reagan, D. Seidov, E. S. Yarosh, and M. M. Zweng, "World ocean heat content and thermosteric sea level change (0–2000 m), 1955–2010," *Geophysical Research Letters*, vol. 39, no. 10, 2012.

[13] C. P. Atkinson, N. A. Rayner, J. J. Kennedy, and S. A. Good, "An integrated database of ocean temperature and salinity observations," *Journal of Geophysical Research: Oceans*, vol. 119, no. 10, pp. 7139–7163, 10 2014.

[14] R. Killick, "Making a data product from ocean profiles – the en4 experience," *Presentation*, 2018.

[15] B. Ingleby and M. Huddleston, "Quality control of ocean temperature and salinity profiles — historical and real-time data," *Journal of Marine Systems*, vol. 65, pp. 158–175, 03 2007.

[16] C. P. Morice, J. J. Kennedy, N. A. Rayner, and P. D. Jones, "Quantifying uncertainties in global and regional temperature change using an ensemble of observational estimates: The hadcrut4 data set," *Journal of Geophysical Research: Atmospheres*, vol. 117, no. D8, 2012.

[17] V. Gouretski and R. Franco, "On depth and temperature biases in bathythermograph data: Development of a new correction scheme based on analysis of a global ocean database," *Deep Sea Research Part I: Oceanographic Research Papers*, vol. 57, pp. 812–833, 06 2010.

[18] K. Trenberth, J. Fasullo, K. Schuckmann, and L. Cheng, "Insights into earth's energy imbalance from multiple sources," *Journal of Climate*, 07 2016.

[19] J. Fasullo, R. Nerem, and B. Hamlington, "Is the detection of accelerated sea level rise imminent?" *Scientific Reports*, vol. 6, p. 31245, 08 2016.

[20] M. Sato, J. E. Hansen, M. P. McCormick, and J. B. Pollack, "Stratospheric aerosol optical depths, 1850-1990," *J. Geophys. Res.*, vol. 98, pp. 22 987–22 994, 1993.

[21] L. Cheng, K. E. Trenberth, J. T. Fasullo, M. Mayer, M. Balmaseda, and J. Zhu, "Evolution of ocean heat content related to enso," *Journal of Climate*, vol. 32, no. 12, pp. 3529–3556, 2019.

[22] C. Domingues, J. Church, N. White, P. Gleckler, S. Wijffels, P. Barker, and J. Dunn, "Improved estimates of upper-ocean warming and multi-decadal sea-level rise," *Nature*, vol. 453, pp. 1090–3, 07 2008.

[23] H. Hátún, A. B. Sandø, H. Drange, B. Hansen, and H. Valdimarsson, "Influence of the atlantic subpolar gyre on the thermohaline circulation," *Science*, vol. 309, no. 5742, pp. 1841–1844, 2005.

[24] M. Meredith, , and Coauthors, "Polar regions. ipcc special report on the ocean and cryosphere in a changing climate, h.-o. pörtner et al., eds. (in press)," *H.-O. Pörtner et al., Eds. (in press)*, 2019.

[25] J. Robson, P. Ortega, and R. Sutton, "A reversal of climatic trends in the north atlantic since 2005," *Nature Geoscience*, vol. 9, 06 2016.

Declaration of Work Undertaken

Most aspects of the work were evenly distributed between my project partner and myself. We decided to share all of our work with each other, but focus on different aspects, to make as much progress as possible. Initially, I focussed on creating maps of the data set to understand what we were given, while my partner calculated the Ocean Heat Content (OHC) at a single point. I extended this calculation to a global sum. In the following weeks we focused on optimising the code to run more efficiently, where both contributed.

While I focused on finding the regional variations on a map, my partner analysed the OHC change by basin. Furthermore, I performed a Monte Carlo analysis of the uncertainties of EN4, while my partner investigated the OHC by depth in different basins. Finally, I added events such as El Niño-Southern Oscillation and volcanic eruptions to my analysis and created a zonal-mean plot, to add the dimension of depth to my regional variation analysis.

Jakob Torben
London, 14/01/2020